Astronomical, Atmospheric, and Lifetime-specific Requirements for Cooling Contrails

Judith Rosenow and Sophie Köhler
Institute of Logistics and Aviation
Technische Universität Dresden
Dresden, Germany
judith.rosenow@tu-dresden.de

***Abstract*—The radiative impact of contrails has posed challenges for both scientists and regulators for decades, as this metric is essential to quantify the influence of air traffic on the greenhouse effect. However, it is clear that, depending on the sun's position and the contrail's lifetime, individual contrails can have a cooling effect on the Earth's atmospheric radiation balance. This study focuses on astronomical conditions with optimal sun positions (preferably during sunrise and sunset), the resulting requirements for contrail lifetimes (two to seven hours), and identifies atmospheric conditions (such as slight updrafts and thin ice-supersaturated layers) that enable the required lifetimes. Analyses of real historical weather data suggest that these conditions occur approximately during 30 % of the year. Consequently, cooling contrails regularly happen, and their radiative impact is likely overestimated. The results of this study can provide valuable insights for predicting and internalizing contrails.**

***Keywords*—Contrail prediction, climate change assessment, Weather data analysis**

I. Introduction

Condensation trails (contrails) are anthropogenic clouds that form behind aircraft as a result of water vapor emissions condensing on soot particles and atmospheric condensation nuclei in a cold environment, meeting the conditions outlined in the Schmidt-Appleman criterion [1], [2]. In an ice-supersaturated (Iss) atmosphere (i.e. relative humidity for ice $rH_{ice} < 1$), these artificial ice clouds can evolve into persistent cirrus clouds, classified as "Cirrus homogenitus" by the World Meteorological Organization [3].

Contrails act as a disruptive factor in the Earth's atmospheric energy budget [4], [5]. They scatter incoming shortwave solar radiation back into space, producing a cooling effect, while also absorbing and re-emitting outgoing longwave terrestrial radiation back toward the Earth's surface, contributing to a warming effect in the lower atmosphere [4], [6]–[8].

The dominating effect, i.e., the instantaneous imbalance of the Earth-Atmosphere energy budget is called radiative forcing RF [$\mathrm{W\,m^{-2}}$]. The radiant power coming from the sun (i.e., the radiant flux) [W] summarizes the total power emitted in the form of solar radiation. If the radiation irradiates a surface (e.g., the Earth or a contrail), this is referred to as the radiant power acting on a defined area (i.e. the ratio of radiant power to the irradiated area) and is referred to as irradiance in [$\mathrm{W\,m^{-2}}$]. The relationship to the area is important, as the same radiation is distributed over a larger area at flat angles of incidence (resulting in smaller irradiation) than with perpendicular irradiation. The angle of incidence is called solar zenith angle θ [°] (see Figure 1). However, solar radiation is not only scattered and absorbed by the contrail; each molecule on Earth and in the atmosphere absorbs and scatters radiation and emits the absorbed radiation according to its new temperature [9]. This results in a long-wave terrestrial radiation spectrum radiating from all spatial directions, which is preferably absorbed by the contrail. Scattered solar radiation by atmospheric molecules results in diffuse solar radiation coming from all directions in space.

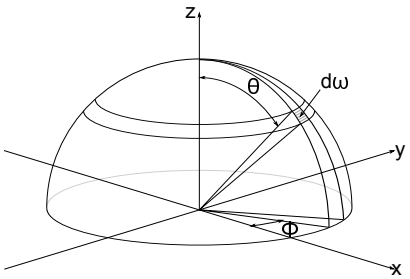

Figure 1. Angles and orientation of polar coordinates. Solar zenith angle θ [°] measures the angle of radiation in the vertical plane.

If this irradiance is extinguished by the contrail and thus the balance between incoming and outgoing radiation is disturbed, radiative forcing occurs. The radiative forcing of individual contrails has been estimated with a physical-optical model in which photons of representative wavelengths are tracked on their path through the contrail from all spatial directions and their efficiencies for scattering (redirection) and absorption are mapped stochastically in a Monte Carlo simulation [10]. In [11] optimal conditions for contrail-induced cooling have been identified at solar zenith angles of $65° < \theta < 80°$, where horizontal photon transport enhances the likelihood of direct solar radiation being scattered into the upper hemisphere. However, as the solar zenith angle increases $\theta > 80°$, the intensity of solar radiation incident on a horizontal contrail surface converges to Zero, which is why $\theta = 90°$ does not maximize the cooling effect.

Photon absorption and backward scattering of radiation originating from the lower hemisphere contribute to a warming effect, which must be counterbalanced by cooling due to the backward scattering of photons from the upper hemisphere.

While terrestrial long-wave radiation, predominantly from the lower hemisphere, is largely absorbed, direct short-wave solar radiation is more likely to be scattered. Due to the dependence on solar zenith angle θ, the solar warming effect, resulting from the scattering and absorption of diffuse solar radiation from all directions, is highly dependent on the type of Earth's surface below the contrail. The solar cooling effect, due to the scattering of direct solar radiation, is strongly influenced by latitude, time of day, and season [11]. Mid and high latitudes have a higher potential for inducing cooling contrails, due to the frequent occurrence of large solar zenith angles in these regions. This observation is further supported by the increased likelihood of contrail formation at these latitudes, which is favorable since a substantial amount of air traffic occurs there. On the other hand, the type of land surface beneath the contrail has a minimal impact, except over snow-covered regions, where the contribution of diffuse solar radiation to the energy budget is less significant compared to the influence of direct solar radiation [11].

If a contrail forms during a large solar zenith angle, there is a good chance that it will cool, at least initially. During its lifetime, however, the position of the sun changes, and there is a risk that the contrail will live longer than the sun irradiates the contrail at an optimum angle. As a result, the warming effect might dominate in the end. The question therefore arises as to how long the sun is at the optimum angle and how long contrails live. These questions are answered in this paper and supplemented by an analysis of real weather data to finally answer the probability of cooling contrails in the mid-latitudes:

1) How long may/must contrails live depending on latitude, time of day, and year to have a cooling effect on the climate balance?
2) Under what atmospheric conditions are such lifetimes possible?
3) Where and how frequently can these atmospheric conditions be found in reality?

To answer the questions, θ is analyzed as a function of latitude, time of the day, and season. Subsequently, a physical contrail life cycle model [12] is applied and parameterized for contrail lifetimes elaborated in the first step. Afterwards, realistic weather data is analyzed for those conditions.

II. State of the Art

A. Individual Contrail Radiative Forcing

Although the radiative forcing of individual contrails has been under investigation for 30 years, there are still major uncertainties to be lamented [13]. Photon-based studies on individual contrails, such as those conducted by Gounou et al. [14] and Forster et al. [15], focused on examining the radiative effects of single contrails, with particular emphasis on the significance of large solar zenith angles at sunrise and sunset. These studies utilized a Monte Carlo code for photon transport on a coarse spatial grid and did not account for the influence of flight performance on the optical properties of contrails. However, phenomena like multiple scattering were considered.

Schumann et al. [16], [17] developed the Contrail Cirrus Prediction tool (CoCiP), an empirical and parametric radiative forcing model designed to calculate the radiative extinction of individual contrails. This model has a low dependency on the solar zenith angle and particle radius, with the time of day reflected only through a weak dependence on the solar zenith angle. The optical properties are parameterized based on radiant fluxes integrated over a hemisphere, which means that the model does not account for angular dependencies related to the time of day or the spatial orientation of the contrail.

Building on Schumann's model, Avila and Sherry [18] assumed a constant optical depth to evaluate the radiative forcing of individual contrails. In their model, the optical depth, width, and particle diameter of contrails are generally parameterized. Schumann's approach involves estimating an effective particle radius for each contrail class, with each radius corresponding to specific optical properties. A notable advantage of Avila and Sherry's study is that it considers the solar zenith angle.

Rosenow [10], [12] conducted detailed investigations in a Monte Carlo Simulation, taking into account all possible solar zenith angles to enable analysis across all times of the day.

On the other hand, promising satellite-based approaches, such as [19], detecting and analyzing contrails and their impact on cirrus cloud formation and climate using satellite data or [20] estimating cloud radiative forcing in contrail clusters using Geostationary Operational Environmental Satellite (GOES) imagery have been further developed by [21] analyzing the properties of linear contrails in the Northern Hemisphere, using data from the Moderate Resolution Imaging Spectroradiometer (MODIS) on NASA's Aqua satellite and [22] utilizing a deep learning algorithm to estimate contrail altitudes based on GOES-16 ABI infrared imagery.

B. Individual Contrail Lifetime

In studies that focus on important features of the contrail lifetime, satellite observations are feasible when contrails are fully developed (specifically during the dissipation phase) [23], [24] and dominate the research field. However, satellite detection is effective only while the contrail maintains its characteristic line-shaped structure as an artificial cirrus cloud in the atmosphere [25]–[28].

Wang et al. [29] further examined the microphysical properties of satellite-observed contrails. Their comparisons of effective radius, particle number density, and optical thickness between contrails, contrail cirrus, and natural cirrus—based on in-situ measurements indicated that contrails have smaller particle radii than natural cirrus clouds.

Another approach uses micro-physical models. For instance, the Contrail Cirrus Prediction (CoCiP) tool models the life cycle of individual contrails as a Gaussian plume [16]. This model describes average contrail particle properties while neglecting interactions with meteorological conditions [16], [30]. Although detailed observations identifying numerous factors affecting contrail lifetime and optical properties, such as local wind speeds, humidity, and wind shear, were published by

Schumann and Heymsfield [30], these factors are not included in the CoCiP model. CoCiP prioritizes short computation times and minimizes the number of input variables.

In-situ [31] and remote-sensing measurements [32] of contrails, while not primarily focused on modeling individual contrail life cycles, offer valuable insights into typical lifetimes and can also be used for model validation. In such studies, research aircraft equipped with cloud microphysics probes and remote-sensing instruments sampled contrails aged between 7 and 30 minutes. Lidar measurements during these flights effectively identified contrail location, size, and some optical properties, outperforming shortwave spectrometer measurements. Subsequent modeling of the contrail life cycle was compared with the UK Met Office's NAME III climate model [33]. Despite their valuable insights, the effort required for such measurements limits their feasibility for long-term studies across all atmospheric conditions influencing contrail lifetimes. Furthermore, using satellite remote sensing data, [34] presented an interesting study of the diurnal variation in high cloudiness induced by aviation, including contrails.

Rosenow extended and validated [12] the Gaussian plume model developed by [16] by particle size distributions according to the available Ice Water Content (IWC), and to the position within the contrail cross-section, by particle shape distributions according to the contrail temperature, by temperature changes due to adiabatic heating and by the existence of overlapping contrails [35]. This model is used in this study.

III. Solar zenith angle

As figured out by [11], the decisive feature for the cooling effect of contrails is the solar zenith angle θ [°] [36]

$$\cos\theta = \sin\Phi\sin\delta + \cos\Phi\cos\delta\cos\omega, \tag{1}$$

as function of the hour angle ω [°] in the local solar time h, the current declination of the sun δ [°], and the local latitude Φ [°]. The hour angle ω describes the angular distance between the meridian and the sun's position longitude:

$$\omega = 15(h - 12) \tag{2}$$

with h the hour of the day. Declination δ is the angle between the solar irradiation and the equatorial plane of the Earth and can be approximated by:

$$\delta \approx \epsilon \sin\left(\frac{360}{365.2422}n\right) \tag{3}$$

where n is the number of days after the first day of spring (i.e., 21^{st} of March) and ϵ is the obliquity of the ecliptic as a function of the Julian century T

$$\epsilon = 23.4392 - 0.013T - 0.01610^{-6}T^2 + 0.510^{-6}T^3 \tag{4}$$

with

$$T = \frac{D - 2451545}{36525} \tag{5}$$

where the Julian Day D is approximated according to Meeus [37] depending on year y, month m, day d and time$t$

$$D = 365.25(y + 4716) + 30.6001(m + 1) + d \tag{6}$$

$$+\frac{t}{24} + 2 - \frac{y}{100} + \frac{y}{400} - 1524.5. \tag{7}$$

From Equations 1-7 follows that θ can be approximated as function of latitude Φ, day of the year (i.e., year y, month m, day d), and time of the day t (see Figure 2).

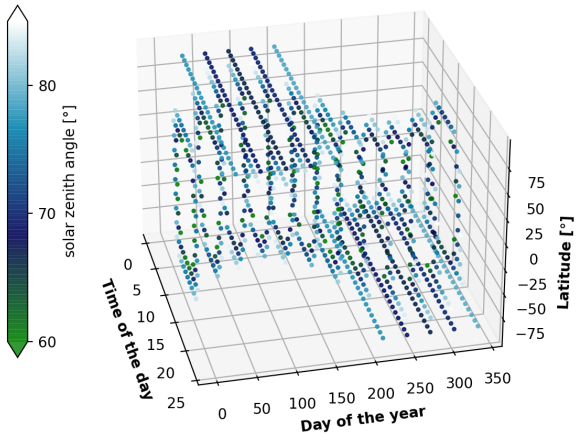

Figure 2. Solar zenith angle $60° < \theta < 85°$as a function of time of the day, time of the year, and latitude. Cooling conditions dominate during sunrise and sunset all over the year. Near the pole facing the sun, θ remains between $65°$and $80°$throughout the day.

In Figure 2 the expected behavior of the sun can be detected: large solar zenith angles occur during sunrise and sunset. Depending on the season, near the pole that is facing the sun, θ consistently remains between $65°$ and $80°$ throughout the day. However, Figure 2 suggests only a short period with $65° \leq \theta \leq 80°$along longitudes with high air traffic volumes. This presumption is confirmed in Figure 3, where θ is shown for $50°$latitude in detail.

Between the end of October (29^{th} of October) and begin of February (6^{th} of February) $60° \leq \theta \leq 85°$is valid for a long period between 4.5 and 7 hours (5.5 hours on average) in a row around noon. During the rest of the year (7^{th} of February to 28^{th} of October) the sun reaches $60° \leq \theta \leq 85°$for only 1 to 2 hours (1.5 hours on average) in the morning and the evening, respectively. From this, contrails do not have much time to cool the atmosphere during the major part of the year. Compared with modeled and observed lifetimes of up to 20 hours, there is a risk of a positive contrail radiative forcing even with contrails formed during sunrise and sunset.

It follows that we want to look for atmospheric conditions under which contrails live for a maximum of 1.5 hours in spring, summer, and fall and a maximum of 5.5 hours in winter.

IV. Contrail Lifetime

For identifying atmospheric conditions enabling short contrail lifetimes, a physical contrail lifetime model is used which

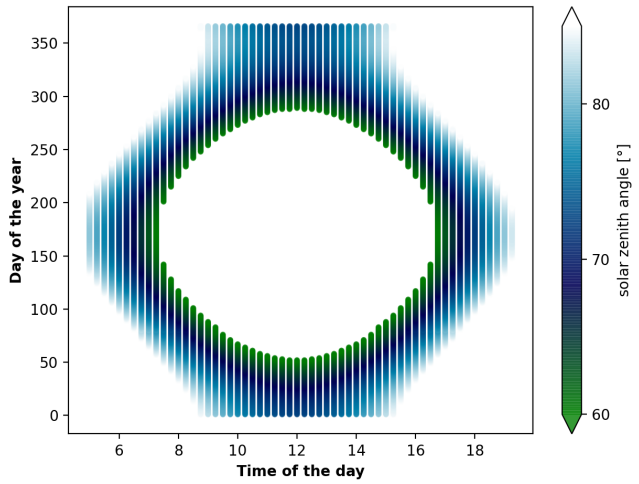

Figure 3. Solar zenith angle $60° \leq \theta \leq 85°$as a function of time of the day and time of the year at $50°$latitude. The cooling conditions dominate during sunrise and sunset all over the year. Near the pole facing the sun, θ remains between $65°$and $80°$throughout the day.

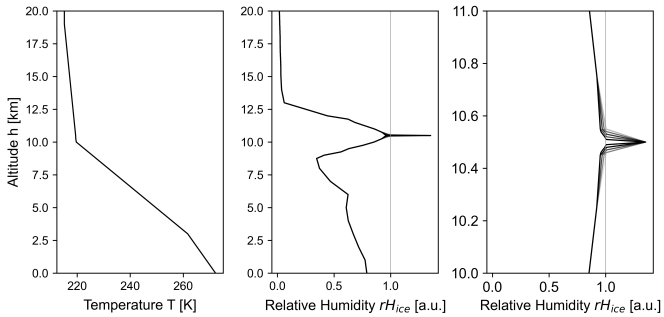

Figure 4. Temperature and humidity (with respect to ice) profile of the model atmosphere AFGLMW. The humidity profile is modified to ensure different vertical depths of ISS.

has been validated with ground-based camera measurements of contrails over Central Europe [12]. For this case study, and for the sake of comparability, a modified version of the Mid-Latitude Winter atmospheric reference model provided by the Air Force Geophysical Laboratory (AFGL) [38] is used and modified in scenarios in order to manipulate the vertical depth of the ISS layer. This model represents average values of temperature, pressure, and density as functions of altitude. Additionally, it provides the concentrations of water vapor (H_2O), ozone (O_3), nitrous oxide (N_2O), carbon monoxide (CO), and methane (CH_4) in terms of volume mixing ratios (ppm) as a function of altitude. The inclusion of water vapor and trace gas concentrations is a distinguishing feature of the AFGL model compared to other standard atmospheres. At typical cruising altitudes, the model is already cold enough to fulfill the Schmidt-Appleman criterion.

To further model the potential of the appearance of persistent contrails in accordance with realistic heterogeneous atmospheric conditions, the relative humidity with respect to ice (rH_{ice}) is manipulated following a Gaussian distribution function with a mean value of $10.5\ \mathrm{km}$ and different values for the standard deviation. Therewith, realistic maximum values of $rh_{\mathrm{ice}} = 1.35$ are achieved [39]. The Gaussian distribution function is used to model a smooth transition between the original values of relative humidity and the manipulated ones. The resultant humidity profiles can be seen in Figure 4. With these manipulations, the contrail life cycle model could be applied to nine different ISS layer thicknesses $d_{\mathrm{rh,ice,i}}$ [m] with an increment of 10 m:

$$d_{\mathrm{rh,ice,i}} \text{ for } i \in \{20, .., 100\}. \tag{8}$$

In general, there are two reasons for a contrail to sublime: First, the air inside the contrail is no longer ice-supersaturated ($rH_{\mathrm{ice}} < 1$), and second the ice particles are too far apart from one another. At this stage, the radiative extinction of the ice particles becomes negligible. The second criterion is considered by the IWC as the total amount of ice mass per volume contrail expressed in $[\mathrm{kg\,m^{-3}}]$. A critical value of $IWC < 10^{-8}\ \mathrm{kg\,m^{-3}}$ has been identified with the help of measurements in real high-altitude cirrus clouds [40].

The contrail life cycle model uses a Gaussian plume model to simulate the turbulent diffusion of the contrail until it is completely mixed with the atmosphere [12]. Therein, contrail ice particles grow because the cross-section of the contrail increases and thus absorbs new ISS air from the environment. However, according to Stokes' law [41], the ice particles are confronted to a viscous friction

$$F_{\mathrm{W,p}} = 6\,\pi\,\eta_{\mathrm{dyn}}\,v_{\mathrm{s,p}}\,r_p. \tag{9}$$

where $F_{\mathrm{W,p}}$ [N] is a drag force, $v_{\mathrm{s,p}}$ $[\mathrm{m\,s^{-1}}]$ is the sedimentation speed of the ice particle, r_p [m] is the radius of the ice particle, ρ_p $[\mathrm{kg\,m^{-3}}]$ is the density of the ice particle, and η_{dyn} $[\mathrm{kg\,m^{-1}s^{-1}}]$ is the dynamic viscosity. $F_{\mathrm{W,p}}$ is balanced by the particle's gravitational force $F_{\mathrm{G,p}}$ [N]:

$$F_{\mathrm{G,p}} = \frac{4}{3}\,\pi\,r_p^3\,\rho_p\,g, \tag{10}$$

Equating Equations 9 and 10 [42] yield the wind-neglecting sedimentation speed $v_{\mathrm{s,p}}$:

$$v_{\mathrm{s,p}} = \frac{2\,r_p^2\,\rho_p\,g}{9\,\eta_{\mathrm{dyn}}}. \tag{11}$$

This sedimentation (which also takes place in every natural cloud) is additionally compensated for by a weak upwind. If the upwind exceeds the sedimentation, the contrail rises until it finally leaves the ISS layer. If the sedimentation exceeds the upwind, the contrail falls out of the ISS layer on the underside.

It follows that the longer the sedimentation of the particles remains largely constant and corresponds to the current upwind, the longer the contrail lives. Furthermore, it can be concluded that the thicker the ISS layer, the longer the contrail remains in the ISS layer and is thus alive despite vertical movement. Inspired by these theoretical considerations [12], two atmospheric conditions are expected to be crucial for the

contrail lifetime. First, the ISS layer thickness ($d_{rH_{\mathrm{ice}}}$) and second the upwind speed v_z. For the second criterion, the upwind speed v_z [$\mathrm{m\,s^{-1}}$] has been varied in 19 steps between

$$v_{z,j} \text{ for } j \in \{10^{-4}, .., 10^{-2}\}. \tag{12}$$

Conversely, in conditions with low ISS, the contrail dissipates due to an $IWC < 10^{-8}$ $\mathrm{kg\,m^{-3}}$, as the ice mass is spread across a larger contrail volume. Additionally, if upwind is weak in a slightly ISS environment, the contrail cannot absorb enough surrounding humidity. Furthermore, a low turbulence level (such as $\varepsilon < 10^{-6}$ $\mathrm{s^2\,m^{-3}}$) causes a slow mixing with the environment, resulting in a small increase in ISS air - and thus a short contrail lifetime.

However, [39] measured the amount of ISS in those regions. They rarely measured values of $rh_{\mathrm{ice}} > 1.4$. From this follows, the worst case (in terms of a long lifetime) is already assumed in this study. The turbulence is already considered in the following way: According to [43], the vertical velocity is a suitable characteristic value of the turbulence, because it highly correlates with the turbulence. This approach for estimating the eddy dissipation rate ε as a measure of turbulence [44] is already implemented in the contrail lifetime model. Since the upwind has already been varied in this study, correlating turbulence variations are also considered. With this variation in input variables, the contrail life cycle model is applied for a contrail induced behind an A320 with a true air speed of 230 $\mathrm{m\,s^{-1}}$ at 10500 m altitude (the altitude with maximum ISS in the model atmosphere, compare Figure 4) assuming a constant wind shear $s = 0.0002$ $\mathrm{s^{-1}}$ as difference in horizontal wind speed between two altitudes. The atmospheric turbulence depends on the upwind speed and varies between $10^{-6} < \varepsilon < 10^{-4}$ $\mathrm{s^2 m^{-3}}$. In the resultant Figure 5, conditions of short contrail lifetimes (up to 1.5 hours) are denoted at blue dots. First, a continuous increase in the lifetime as a function of the ISS layer thickness can be seen.

Furthermore, an upwind speed of $v_z = 0.004$ $\mathrm{m\,s^{-1}}$ maximizes the lifetime for all ISS layer thicknesses. Obviously, the particle sedimentation, which is counteracted by the upwind is in this range for a long period of the contrail lifetime. So contrail stays the maximum time in the ISS layer. This assumption is confirmed in the Figure 6. This statement, however, is related to the chosen degree of ice-supersaturation ($rH_{\mathrm{ice,max}} = 1.35$ in this study, validated by [39]).

From Figure 5 follows, ISS thicknesses greater than 100 m do not enable lifetimes shorter than 1.5 hours. Upwind speeds greater than 0.01 $\mathrm{m\,s^{-1}}$ will always quickly updrift the contrail outside the ISS layer. Upwind speeds smaller than 0.0009 $\mathrm{m\,s^{-1}}$ will not ensure the existence of the ISS layer, since clouds can only survive in upwind situations.

A. Validation of calculated Contrail Lifetimes

With maximum values of 14 hours, Figure 5 indicates atmospheric conditions causing a much longer lifetime than 1.5 or 5.5 hours. For this reason, several kinds of contrail observations are used to compare the calculations with real

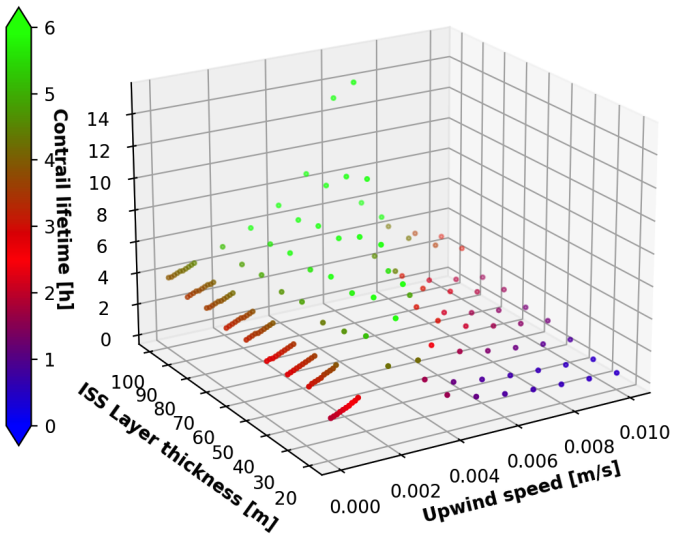

Figure 5. Contrail lifetime as a function of upwind speed and ISS thickness layer. Blue points indicate lifetimes up to 1.5 hours for days, where $65 < \theta < 80$ is only valid during sunrise and sunset. Red points indicate lifetimes up to 5.5 hours, where $65 < \theta < 80$ is valid near the poles during a very short day. Green points indicate lifetimes longer than 5.5 hours.

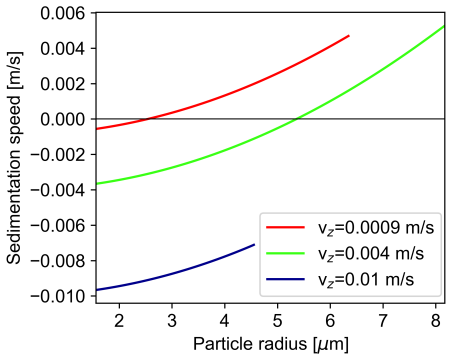

Figure 6. Ice particle sedimentation speed as a function of ice particle radius under various upwind conditions. For upwinds of $v_z = 0.004$ m/s (green), ice particles sink for about as long as they subsequently rise. For upwinds $v_z < 0.004$ m/s (red) ice particles mainly rise, and for $v_z > 0.004$ m/s (blue) ice particles mainly sediment.

contrails. For example, [45] analyzed 1778 contrail recordings from formation until sublimation using their ground camera-based system above the Czech Republic. 284 of them were persistent and had an average lifetime of 6.2 minutes with maximum values of around 50 minutes. In addition to the 284 analyzed contrails, they observed 177 persistent contrails that left the field of view after 50 minutes at the latest during their diffusion, i.e. whose lifespan could not be determined. The fixed viewing angle of the cameras does not allow to follow contrails drifting out of the camera's field of view. From this follows that much longer living contrails were observed with this camera system. Additionally, it can be concluded that contrails do not only vertically shift, but also horizontally drift with the wind. In this case study, for comparability, a 1D model atmosphere was used and horizontal wind drift was

neglected. This assumes an infinitely extended ISS layer in the horizontal plane, which does not correspond to realistic conditions. However, high-resolution information on the dimensions of ISS areas is scarce.

The modeled contrails can also be compared to remote-sensing observations that have been conducted since 1975 [46]. The sizes and lifespans of the modeled contrails are consistent with those observed in studies by [47], who observed contrails with geostationary satellite data that lived between 7 and 17 hours [26], [48]. However, observations of longer-lasting contrails show that they tend to have extended lifetimes [49].

Additionally, Large Eddy Simulations of contrails [50], despite having a relatively coarse temporal and spatial resolution, produce results that are comparable to those of the current model.

V. Real Weather Data Analysis

After the modeled contrail lifetime was considered realistic based on real measurements from the literature, the identified upwinds and ISS layer thicknesses for short lifetimes should now be compared with real atmospheric conditions. Compared to spare 3D measurements of the relative humidity, the vertical wind is measured and modeled by nearly all weather prediction models. For this reason, realistic weather data, used for numerical weather predictions could be analyzed on a sufficiently large scale. For example, Figure 7 quantifies the probability of the identified small upwind speeds $10^{-4}, .., 10^{-2}$ m/s as a function of latitude between 12 % and 35 % in April 2023. For this purpose, 777600 samples from different northern latitudes between $20°$ and $70°$ at usual flight levels were analyzed four times a day on all 30 days in April 2023 with a resolution of $0.5°$ and integrated over all longitudes. Thereby, an impact of the longitude could not be identified (see Figure 9).

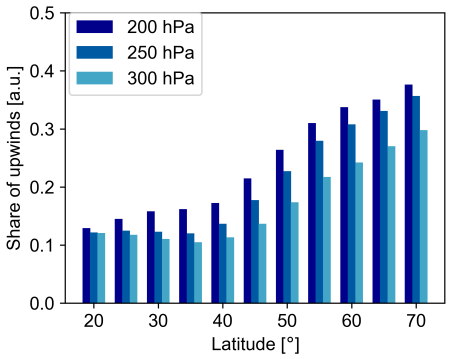

Figure 7. Probability of upwind speeds $10^{-4} \leq v_z \leq 10^{-2}$ m/s in modelled weather data in April 2023 provided by the Global Forecast System (GFS) as function of latitude and altitude. As expected, the amount of small upwind speeds increases with distance from the Hadley cell (i.e. latitude).

With Figure 7 it can can be demonstrated that in April 2023 the upwind condition for short contrail life times was fulfilled with a probability of 15 to 30 % in the northern latitudes showing an increasing tendency with increasing altitude. Furthermore, following the global circulation model of a Hadley cell, strong vertical movements are expected in low latitudes due to high surface temperatures. From this follows, the probability of small upwind speeds increases with increasing distance from the Equator.

However, Figure 7 only concentrates on a single-month analysis and may be biased by seasonal effects. For this reason, the whole year 2023 has been analysed on three days per month during sunrise and sunset (to ensure large solar zenith anlges). In total 15.707.520 data points were checked. In Figure 8, both the condition of ISS and upwinds $v_z \notin [0.0035, 0.0045]$ m/s (resulting in large lifetimes, see Figure 5) have been added to the criterion for the probability of occurrence.

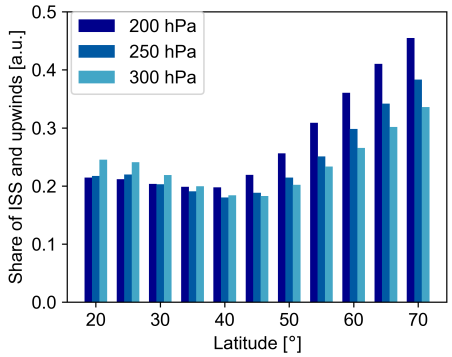

Figure 8. Probability of upwind speeds $10^{-4} \leq v_z \leq 10^{-2}$ m/s and $v_z \notin [0.0035, 0.0045]$ m/s in ISS regions modelled on the 1st, 7th, and 15th day of each month in 2023 at 6 a.m. and 6 p.m. provided by the GFS as function of latitude and altitude, integrated over all longitudes.

Surprisingly, over the year the probability of the desired conditions increases, compared to the analysis of a single month. With a probability of occurrence of 30 % it can be shown that both the investigated upwind range was chosen realistically and that the identified conditions for short contrail lifetimes occur almost every third day during sunrise or sunset in the northern hemisphere.

Due to the limited vertical resolution of 50 hPa (corresponding to $\approx$ 1000 m, i.e., $\approx$ 3280 ft, i.e., 3 different flight levels) of the modeled weather data, an elaboration on the vertical thickness of ISS layers is impossible. For this reason, again, measurements from the literature were taken into account. In 2009, Dickson et al. [51] published an analysis over five years of radiosonde measurements coming from nine measurement stations all over the globe and found that 27 % to 34 % of ISS layers are less than 100 m deep. This totally corresponds to the assumptions taken in this study. Furthermore, [39] analyzed humidity profiles (measured by aircraft) from the Measurement of OZone by Airbus In-service airCraft (MOZAIC) champagne in the northern mid-latitudes and found probabilities for the occurrence of ISS layers around the tropopause of 20 % to 30 %. Again, these measurements agree with the analysis of weather data shown in Figure 8. Unfortunately, neither layer thickness, nor their horizontal dimension could be evaluated here, as measurements were

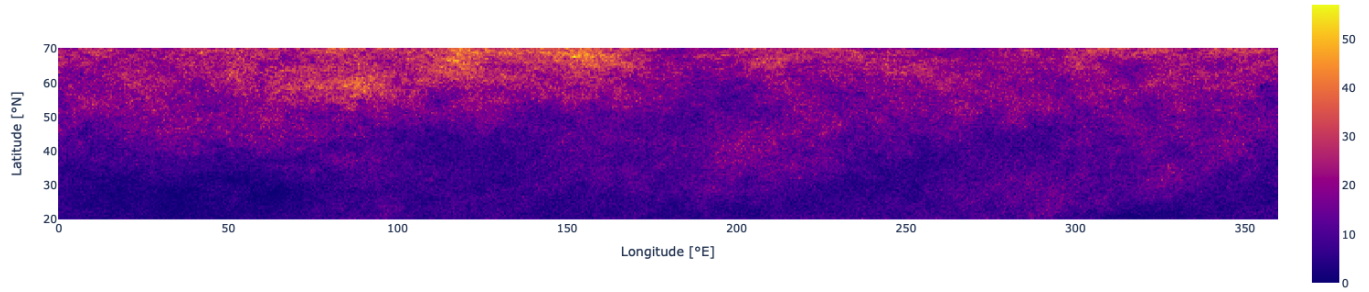

Figure 9. Probability of upwind speeds $10^{-4} \leq v_z \leq 10^{-2}$ m/s summarized over three days per month in 2023 (36 days in total) and over three pressure level (200, 250 and 300 hPa). Obvioulsy, there is no dependence on laongitude.

evaluated in flight (i.e., along a single path).

Most important, however, seems an analysis of the size and distribution of ISS layers within the In-service Aircraft for a Global Observing System (IAGOS) project that mainly found small horizontal dimensions (in the order of 10 km) that can easily be left by the contrail [52] with an important impact on a short contrail lifetime, as discussed in Section IV.

VI. Conclusions and Outlook

In this study, time windows with optimal astronomical conditions for cooling contrails were compared with atmospheric conditions for corresponding short-lived contrails and compared with real weather analyses. Despite surprisingly short time windows with optimal astronomical conditions during large parts of the year, atmospheric conditions could be identified (i.e., low ISS layer thickness and small upwinds) that allow such short-lived contrails and occur during 30 % of the year in northern latitudes. Since contrails only form in ISS regions and only in upwind conditions, probability of a short-lived contrail, if one occurs, is approximated to 30 %. This is more frequently than expected, when the study was initiated.

However, the study suffers from two weaknesses, which will be rectified shortly. Firstly, for reasons of comparability, the lateral expansion of ISS regions and thus the possibility of contrails drifting laterally out of the regions was neglected. This is assumed to result in an artificial extension of the lifetime. This would extend the atmospheric conditions for short contrail lifetimes. On the other hand, the vertical thickness of the ISS region could not be thoroughly validated. However, this is decisive for a short contrail lifetime, at least if lateral drift is neglected.

There are two solutions to this problem. Firstly, large quantities of radiosonde data sets, which cover both lateral drift and relative humidity, can be fed into the lifecycle model to get closer to reality. On the other hand, intelligent interpolation approaches such as Kriging or Meteo Particle can be applied to weather data sets with the highest possible resolution, presumably modeled locally, in order to create a four-dimensional image of the atmosphere.

Acknowledgments

This research is part of the project ICATO (Individual Condensation trails in Aircraft Trajectory Optimization) founded at the TU Dresden Chair of Air Transport Technology and Logistics by Judith Rosenow. The authors would like to thank Hartmut Fricke for hosting the Chair of Air Transport Technology and Logistics.

References

[1] E. Schmidt, "Die entstehung von eisnebel aus den auspuffgasen von flugmotoren," *Schriften der Deutschen Akademie der Luftfahrtforschung, Verlag R. Oldenbourg, München/Berlin*, vol. 44, pp. 1–15, 1941.

[2] H. Appleman, "The formation of exhaust condensation trails by jet aircraft," *Bulletin of the American Meteorological Society*, vol. 34, pp. 14–20, 1953.

[3] World Meteorological Organization, "Cloud atlas," *https://cloudatlas.wmo.int/aircraft-condensation- trails.html*, 2018. [Online]. Available: https://cloudatlas.wmo.int/aircraft-condensation-trails.html

[4] G. Myhre, D. Shindell, F.-M. Bréon, W. Collins, J. Fuglestvedt, J. Huang, D. Koch, J.-F. Lamarque, D. Lee, B. Mendoza, T. Nakajima, A. Robock, G. Stephens, T. Takemura, and H. Zhang, "Anthropogenic and natural radiative forcing. in: Climate change 2013: The physical science basis. contribution of working group i to the fifth assessment report of the intergovernmental panel on climate change," *Cambridge University Press*, 2013.

[5] D. S. Lee, D. W. Fahey, P. M. Forster, P. J. Newton, R. C. Witt, L. L. Lim, B. Owen, and R. Sausen, "Aviation and global climate change in the 21st century," *Atmospheric Environment*, vol. 43, pp. 3520–3537, 2009.

[6] P. Minnis, U. Schumann, D. R. Doelling, K. M. Gierens, and D. W. Fahey, "Global distribution of contrail radiative forcing," *Geophysical Research Letters*, vol. 26, pp. 1853–1856, 1999.

[7] R. Sausen, I. Isaksen, V. Grewe, D. Hauglustaine, D. S. Lee, G. Myhre, M. Köhler, G. Pitari, U. Schumann, F. Stordal, and C. Zerefos, "Aviation radiative forcing in 2000: An update on ipcc (1999)," *Meteorologische Zeitschrift*, vol. 14, pp. 555–561, 2005.

[8] U. Burkhardt and B. Kärcher, "Global radiative forcing from contrail cirrus," *Nature Climate Change*, vol. 1, pp. 54–58, 2011.

[9] W. Wien, "Xxx. on the division of energy in the emission-spectrum of a black body," *The London, Edinburgh, and Dublin Philosophical Magazine and Journal of Science*, vol. 43, no. 262, pp. 214–220, 1897. [Online]. Available: https://doi.org/10.1080/14786449708620983

[10] J. Rosenow, "Optical properties of condenstation trails," Ph.D. dissertation, Technische Universität Dresden, 2016.

[11] J. Rosenow and H. Fricke, "When do contrails cool the atmosphere?" in *SESAR Innovation Days (SID 2022)*, 2022, Budapest, Hungary. [Online]. Available: https://www.researchgate.net/publication/366905171_When_do_contrails_cool_the_atmosphere

[12] J. Rosenow, J. Hospodka, S. Lán, and H. Fricke, "Validation of a contrail life-cycle model in central europe," *Sustainability*, vol. 15, no. 11, 2023. [Online]. Available: https://www.mdpi.com/2071-1050/15/11/8669

[13] H. Lee and J. R. (eds.), "Climate change 2023: Synthesis report. contribution of working groups i, ii and iii to the sixth assessment report of the intergovernmental panel on climate change," Cambridge University Press, Tech. Rep., 2023.

[14] A. Gounou and R. J. Hogan, "A sensitivity study of the effect of horizontal photon transport on the radiative forcing of contrails," *Journal of Atmospheric Sciences*, vol. 64, pp. 1706–1716, 2007.

[15] L. Forster, C. Emde, B. Mayer, and S. Unterstrasser, "Effects of three-dimensional photon transport on the radiative forcing of realistic contrails," *American Meteorological Society*, pp. 2243–2255, 2011.

[16] U. Schumann, "A contrail cirrus prediction tool," in *Intern. Conf. on transport, Atmosphere and Climate, DLR/EUR, Aachen and Maastricht, 22-25 June*, 2009.

[17] U. Schumann, B. Mayer, K. Graf, and H. Mannstein, "A parametric radiative forcing model for contrail cirrus," *American Meteorological Society*, vol. 51, pp. 1391–1405, 2012.

[18] D. Avila and L. Sherry, "Method for calculating net radiative forcing from contrails from airline operations," in *2017 Integrated Communications Navigation and Surveillance (ICNS) Conference*, ser. DOI: 10.1109/ICNSURV.2017.8011927, 2017.

[19] P. Minnis, J. K. Ayers, R. Palikonda, and D. Phan, "Contrails, cirrus trends, and climate," *Journal of Climate*, vol. 17, no. 8, pp. 1671 – 1685, 2004. [Online]. Available: https://journals.ametsoc.org/view/journals/clim/17/8/1520-0442_2004_017_1671_cctac_2.0.co_2.xml

[20] D. P. Duda, P. Minnis, and L. Nguyen, "Estimates of cloud radiative forcing in contrail clusters using goes imagery," *Journal of Geophysical Research: Atmospheres*, vol. 106, no. D5, pp. 4927–4937, 2001. [Online]. Available: https://agupubs.onlinelibrary.wiley.com/doi/abs/10.1029/2000JD900393

[21] S. T. Bedka, P. Minnis, D. P. Duda, T. L. Chee, and R. Palikonda, "Properties of linear contrails in the northern hemisphere derived from 2006 aqua modis observations," *Geophysical Research Letters*, vol. 40, no. 4, pp. 772–777, 2013. [Online]. Available: https://agupubs.onlinelibrary.wiley.com/doi/abs/10.1029/2012GL054363

[22] V. R. Meijer, S. D. Eastham, I. A. Waitz, and S. R. Barrett, "Contrail altitude estimation using goes-16 abi data and deep learning," *EGUsphere*, vol. 2024, pp. 1–25, 2024.

[23] M. Vázquez-Navarro, H. Mannstein, and B. Mayer, "An automatic contrail tracking algorithm," *Atmospheric Measurement Techniques*, vol. 3, pp. 1089–1101, 08 2010.

[24] H. Mannstein, M. Vázquez-Navarro, K. Graf, D. Duda, and U. Schumann, "Contrail detection in satellite images," *Atmospheric Physics: Background - Methods - Trends*, pp. 433–, 07 2012.

[25] G. Zhang, J. Zhang, and J. Shang, "Contrail recognition with convolutional neural network and contrail parameterizations evaluation," *SOLA*, vol. 14, pp. 132–137, 2018.

[26] D. P. Duda, S. T. Bedka, P. Minnis, D. Spangenberg, K. Khlopenkov, T. Chee, and W. L. Smith Jr., "Northern hemisphere contrail properties derived from terra and aqua modis data for 2006 and 2012," *Atmospheric Chemistry and Physics*, vol. 19, no. 8, pp. 5313–5330, 2019. [Online]. Available: https://acp.copernicus.org/articles/19/5313/2019/

[27] K. McCloskey, S. Geraedts, C. Van Arsdale, and E. Brand, "A human-labeled landsat-8 contrails dataset," in *ICML 2021 Workshop on Tackling Climate Change with Machine Learning*, 2021. [Online]. Available: https://www.climatechange.ai/papers/icml2021/2

[28] V. R. Meijer, L. Kulik, S. D. Eastham, F. Allroggen, R. L. Speth, S. Karaman, and S. R. H. Barrett, "Contrail coverage over the united states before and during the covid-19 pandemic," *Environmental Research Letters*, vol. 17, no. 3, p. 034039, mar 2022. [Online]. Available: https://dx.doi.org/10.1088/1748-9326/ac26f0

[29] Z. Wang, L. Bugliaro, T. Jurkat-Witschas, R. Heller, U. Burkhardt, H. Ziereis, G. Dekoutsidis, M. Wirth, S. Groß, S. Kirschler, S. Kaufmann, and C. Voigt, "Observations of microphysical properties and radiative effects of contrail cirrus and natural cirrus over the north atlantic," *Atmospheric Chemistry and Physics Discussions*, vol. 2022, pp. 1–36, 2022. [Online]. Available: https://acp.copernicus.org/preprints/acp-2022-537/

[30] U. Schumann and A. Heymsfield, "On the lifecycle of individual contrails and contrail cirrus," *AMS Meteorological Monographs*, vol. 58, 01 2017.

[31] H. M. Jones, J. Haywood, F. Marenco, D. O'Sullivan, J. Meyer, R. Thorpe, M. W. Gallagher, M. Krämer, K. N. Bower, G. Rädel, A. Rap, A. Woolley, P. Forster, and H. Coe, "A methodology for in-situ and remote sensing of microphysical and radiative properties of contrails as they evolve into cirrus," *Atmospheric Chemistry and Physics*, vol. 12, no. 17, pp. 8157–8175, 2012. [Online]. Available: https://acp.copernicus.org/articles/12/8157/2012/

[32] J. Spinhirne, W. Hart, and D. Duda, "Evolution of the morphology and microphysics of contrail cirrus from airborne remote sensing," *Geophysical Research Letters - GEOPHYS RES LETT*, vol. 25, pp. 1153–1156, 04 1998.

[33] A. Rap, P. M. Forster, J. M. Haywood, A. Jones, and O. Boucher, "Estimating the climate impact of linear contrails using the uk met office climate model," *Geophysical Research Letters*, vol. 37, no. 20, 2010. [Online]. Available: https://agupubs.onlinelibrary.wiley.com/doi/abs/10.1029/2010GL045161

[34] K. Graf, U. Schumann, H. Mannstein, and B. Mayer, "Aviation induced diurnal north atlantik cirrus cover cycle," *Geophysical Research Letters*, vol. 39, p. L16804, 2012.

[35] J. Rosenow and M. Luo, "Impact of intersected contrails on their lifetime," *Aerospace*, 2024.

[36] H. M.Woolf, "On the computation of solar elevation angles and the determination of sunrise and sunset times," *NASA Technical Memorandu, Washington, D.C.*, vol. 3, pp. X–1646, 04 1968.

[37] J. Meeus, *Astronomical Algorithms*. Willman-Bell, 1998.

[38] G. Anderson, S. Clough, F. Kneizys, J. Chetwynd, and E. Shettle, "Afgl atmospheric constituent profiles (0-120 km)," Air Force Geophys. Lab., Hanscom Air Force Base, Technical Report AFGL-TR-86-0110, 1986.

[39] A. Petzold, P. Neis, M. Rütimann, S. Rohs, F. Berkes, H. G. J. Smit, M. Krämer, N. Spelten, P. Spichtinger, P. Nédélec, and A. Wahner, "Ice-supersaturated air masses in the northern mid-latitudes from regular in situ observations by passenger aircraft: vertical distribution, seasonality and tropospheric fingerprint," *Atmospheric Chemistry and Physics*, vol. 20, no. 13, pp. 8157–8179, 2020. [Online]. Available: https://acp.copernicus.org/articles/20/8157/2020/

[40] A. Afchine, C. Rolf, A. Costa, N. Spelten, M. Riese, B. Buchholz, V. Ebert, R. Heller, S. Kaufmann, A. Minikin, C. Voigt, M. Zöger, J. Smith, P. Lawson, A. Lykov, S. Khaykin, and M. Krämer, "Ice particle sampling from aircraft – influence of the probing position on the ice water content," *Atmospheric Measurement Techniques*, vol. 11, no. 7, pp. 4015–4031, 2018. [Online]. Available: https://amt.copernicus.org/articles/11/4015/2018/

[41] G. G. Stokes, "On the effect of internal friction of fluids on the motion of pendulums," *Transactions of the Cambridge Philosophical Society*, vol. 9, no. part ii, 1851.

[42] W. Roedel, *Physik unserer Umwelt, die Atmosphäre*. Springer-Verlag Berlin Heidelberg, 2000.

[43] R. D. Sharman, L. B. Cornman, G. Meymaris, and J. Pearson, "Description and derived climatologies of automated in situ eddy-dissipation-rate reports of atmospheric turbulence," *Journal of Applied Meteorology and Climatology*, vol. 53, 2014.

[44] R. D. Sharman and J. M. Pearson, "Prediction of energy dissipation rates for aviation turbulence. part i: Forecasting nonconvective turbulence," *Journal of Applied Meteorology and Climatology*, vol. 56, 2017.

[45] S. Lán and J. Hospodka, "Contrail lifetime in context of used flight levels," *Sustainability*, vol. 14, no. 23, 2022. [Online]. Available: https://www.mdpi.com/2071-1050/14/23/15877

[46] H. Hoshizaki, L. B. Anderson, R. J. Conti, N. Farlow, J. W. Meyer, T. Overcamp, K. O. Redler, and V. Watson, *Aircraft wake microscale phenomena*. Department of Transportation, Climatic Impact Assessment Program: A. J. Grobecker, 1975, pp. 2–1—-2–79.

[47] P. Minnis, D. F. Young, D. P. Garber, L. Nguyen, W. L. Smith Jr., and R. Palikonda, "Transformation of contrails into cirrus during success," *Geophysical Research Letters*, vol. 25, no. 8, pp. 1157–1160, 1998. [Online]. Available: https://agupubs.onlinelibrary.wiley.com/doi/abs/10.1029/97GL03314

[48] R. Sussmann and K. M. Gierens, "Lidar and numerical studies on the different evolution of vortex pair and secondary wake in young contrails," *J. Geophys. Res.*, vol. 104, pp. 2131–2142, 1999.

[49] D. Atlas, Z. Wang, and D. Duda, "Contrails to cirrus—morphology, microphysics, and radiative properties," *Journal of Applied Meteorology and Climatology - J APPL METEOROL CLIMATOL*, vol. 45, pp. 5–19, 01 2006.

[50] A. Chlond, "Large-eddy simulation of contrails," *Journal of Atmospheric Sciences*, vol. 55, pp. 796–819, 1997.

[51] N. Dickson, K. Gierens, H. Rogers, and R. Jones, "Vertical spatial scales of ice supersaturation and probability of ice supersaturated layers in low resolution profiles of relative humidity," in *TAC-2 Proceedings, June 22nd to 25th, 2009, Aachen and Maastricht*, 2009.

[52] P. Reutter, P. Neis, S. Rohs, and B. Sauvage, "Ice supersaturated regions: properties and validation of era-interim reanalysis with iagos in situ water vapour measurements," *Atmospheric Chemistry and Physics*, vol. 20, no. 2, pp. 787–804, 2020. [Online]. Available: https://acp.copernicus.org/articles/20/787/2020/